Journal of Marine Science and Technology

Volume 31 | Issue 4 Article 7

Geohash-based Arrangement of Live-Fire Exercise Areas Using AIS

Sang-Lok Yoo
Future Ocean Information Technology, Jeju, Republic of Korea

Cho-Young Jung
. Department of Marine Science and Production, Kunsan National University, Gunsan, Jeonbuk, Republic of Korea, wjdchdud@kunsan.ac.kr

Recommended Citation
Yoo, Sang-Lok and Jung, Cho-Young (2023) "Geohash-based Arrangement of Live-Fire Exercise Areas Using AIS," *Journal of Marine Science and Technology*: Vol. 31: Iss. 4, Article 7.
DOI: 10.51400/2709-6998.2714
Available at: https://jmstt.ntou.edu.tw/journal/vol31/iss4/7

RESEARCH ARTICLE

Geohash-based Arrangement of Live-fire Exercise Areas Using AIS

Sang-Lok Yoo [a], Cho-Young Jung [b,*]

[a] Future Ocean Information Technology, Jeju, Republic of Korea
[b] Department of Marine Science and Production, Kunsan National University, Gunsan, Jeonbuk, Republic of Korea

Abstract

Live-fire exercise (LFX) areas at sea threaten the safety of ships, whereas, and indiscriminately abandoned unexploded bombs threaten the lives of fishermen. No statistical or scientific research has been conducted on the appropriate locations for LFX areas. Therefore, this study proposes a method for effectively arranging the LFX areas at sea that considers the safety of passing ships and national security. First, the proposed method classifies ship tracking data collected in the daytime based on the dawn and dusk times of the civil twilight phase. Second, the method uses a Geohash geocoding process to identify whether an LFX area coincides with the daytime traffic area of the vessels. Finally, a grid search was conducted, in which the polygons of the LFX areas that required rearrangement were shifted by appropriately setting the search range. The methodology presented in this study can be used as a guideline for designing safe LFX areas at sea.

Keywords: Geohash, Grid search, Live-fire exercise area, Arrangement, AIS

1. Introduction

The live-fire exercise (LFX) areas are used by military strategists worldwide to simulate war scenarios that could occur in the real world at sea, on land, and in air. These live-fire military exercises not only provide participating operators with a live shooting experience but also show potential opponents the effective military capabilities the country possesses in the event of conflict [1]. An LFX can involve various weapons and tactics, including small arms, artillery, missiles, torpedoes, anti-ship weapons, multiple warships, aircraft, and other military assets working together to achieve specific goals. Generally, LFXs are important for military forces to maintain their combat readiness and effectiveness. However, an LFX must be performed with adequate security measures to protect the personnel and equipment involved during the operation [1].

Various countries, such as the United States [2], China [3–5], Russia [3,4], Belgium [2], South Korea [6], Denmark [2], Japan [7], France [2], Germany [2], Italy [2], the Netherlands [2], Norway [2], Spain [2], the United Kingdom [2], and etc. usually conduct LFXs to showcase their military potential to the rest of the world [2–7].

In LFX areas located at sea, the navy conducts artillery firing exercises that deploy shells to specific targets from various weapons mounted on destroyers, frigates, and high-speed ships [8]. Additionally, the air force conducts shooting drills by setting specific targets at sea, for fighter jets and helicopters to engage with air grenades, machine guns, and missiles. Therefore, ensuring the safety of these LFX areas is important. In these areas, marine workers may be endangered by unexploded bombs and debris that are indiscriminately deployed away from LFX areas. In addition, fishermen fear losing their productive fishing territories, which are the

Received 7 February 2023; revised 17 October 2023; accepted 18 October 2023.
Available online 15 December 2023

* Corresponding author.
E-mail addresses: sanglokyoo@gmail.com (S.-L. Yoo), wjdchdud@kunsan.ac.kr (C.-Y. Jung).

https://doi.org/10.51400/2709-6998.2714

source of their livelihood. Unexploded ordnances generated during LFXs are dumped into the sea [9–12], which lead to explosion accidents during the net-raising process conducted by fishermen and result in significant casualties.

Moreover, several LFX areas coincide with the main routes for cargo, passengers, and fishing vessels. Accordingly, these LFX areas threaten the safety of passing ships, and unexploded bombs threaten the lives of fishermen. In addition, although vessels are notified of the LFX coordinates in advance through navigation warnings, there is a risk that the navigating vessels will overlook these notifications and sail according to their scheduled route plans. For example, in June 2021, a shell fired by a naval vessel in the waters near Ulleungdo Island, South Korea, fell into the bow and starboard of a passenger ship navigating a regular route, causing a situation that almost resulted in a large number of fatalities.

The literature review conducted in this investigation indicated that in-depth research on the location of LFX areas have not yet been conducted. In this regard, it is important to study the proper arrangement of LFX areas to guarantee maximum fishing rights and safe passage of vessels through LFX areas. It is also necessary to ensure that the minimum conditions for LFX that are essential for national security are satisfied. In this sense, the objective of this study was to propose a method effectively arranging LFX at sea, considering the safety of passing ships and national security.

In this study, an automatic identification system (AIS) was used to determine the latitude, longitude, speed, course, date, and time of reception of each vessel. Then, the Astral Python package and Geohash geocode system were used to extract the vessel traffic-concentrated areas and identify the main traffic flows where the vessels were concentrated [13–15]. Using this information, we can estimate the coincidence rates and detect whether the existing LFX areas coincide with the concentrated areas of vessel traffic. Based on these data, areas with a coincidence rate greater than a threshold were relocated to the location with the lowest coincidence rate in the search range.

This paper proposed a methodology for organizing safe LFX areas at sea. According to this methodology, the ship tracking data collected during the day were classified according to the sunrise and sunset times of the civil twilight phase. Subsequently, using the Geohash geocoding process, the proposed method identifies whether an LFX area coincides with the daytime traffic areas of ships. Finally, a grid search was performed, in which the polygons of the LFX areas that required rearrangement were changed at intervals by appropriately setting the search range. The results show that the coincidence reduction rate of the proposed method is higher than 27 %.

The remainder of this paper is organized as follows: Related studies are reviewed in section 2. Section 3 describes the methodology of the study. Section 4 presents the results of the study and discussion on the results. Finally, section 5 summarizes and concludes the paper.

2. Related studies

Recently, the marine spatial planning (MSP) has been established worldwide, and spatial management has been promoted via legal systematization [16–19]. Põnarbaşõ et al. [20] used the UNESCO MSP database to analyze the sea area usage and scope of MSP. Guerreiro [21] investigated the governance of global MSP and suggested country specific legal and institutional competent departments and application stages. In general, the MSP is used in different settings, such as offshore wind farms, mineral resource development zones, and space utilization in LFX areas. However, the MSP has not conducted studies on the relocation of LFX areas coinciding with commercial vessel passage routes.

Considering previous studies related to shooting training sites, most researchers have focused on environmental pollution and noise. First, considering environmental pollution research cases, Lee [22] conducted an environmental impact assessment by collecting seawater and seafloor sediments around an LFX area and analyzed the presence of marine pollution. Jung et al. [23] studied environmental management guidelines considering soil scrutiny and active soil purification for military shooting ranges. Additionally, Lee et al. [24] conducted a comprehensive examination of noise reduction by installing soundproof walls by synthesizing insights from previous studies concerning mitigating noise from military range operations.

On the other hand, Baek et al. [25] analyzed the characteristics of vessel distribution near the sea LFX areas. They suggested reducing the test volume during the fall season and in the morning to reduce the probability of fishing vessels being exposed to live ammunition. However, this study did not consider the arrangement of the underlying LFX areas.

Finally, to the best of our knowledge, neither other authors nor the MSP have conducted studies on the relocation of LFX areas that coincide with passing vessel areas.

Therefore, in this study, we propose a Geohash-based arrangement for a live-fire exercise area using information provided by the AIS [26,27]. In this regard, Geohash is commonly employed in geospatial applications, such as geolocation and mapping, as it efficiently performs spatial aggregation analysis. Moreover, Geohash is used to index and search for locations in large datasets, such as those provided by the AIS [26,27]. This technique has been used to accurately identify and analyze ship positions using a geohash-based AIS [26−29].

3. Methodology

The following methodological procedure was followed to detect whether the existing LFX areas coincided with concentrated vessel traffic areas. In summary, based on our procedure, we extracted the vessel traffic-concentrated areas and identified the main traffic flows where the vessels were concentrated using the Astral Python package and Geohash geocode system. Then, the accumulated distance traveled by the vessels in each geohash grid was calculated. By combining these two pieces of information, we can estimate the coincidence rates and detect whether existing LFX areas coincide with the concentrated areas of vessel traffic. Finally, the areas with a coincidence rate greater than a threshold value are relocated to the location with the lowest coincidence rate in the search range. The details of this procedure are stated as follows.

3.1. Extraction of the vessel traffic-concentrated areas

Generally, LFX is conducted at sea during the daytime. Therefore, to obtain data on the vessels sailing during the daytime, tracking data were extracted based on the reception date of each vessel and sunrise and sunset times at any latitude and longitude. This information was provided by an automatic identification system (AIS) through the GPS systems installed on the ships.

A previous study shows that sunrise and sunset times vary according to the civil, nautical, and astronomical twilight phases [30]. According to a previous study, civil twilight occurs when the center of the sun lies between the horizon and 6° below it. Therefore, civil dawn twilight begins when the geometric center of the sun is 6° below the horizon and ends at sunrise. Similarly, evening civil twilight starts at sunset and ends when the geometric center of the sun is 6° below the horizon. In other words, civil dawn twilight is the time from 30 min before sunrise to 30 min after sunrise, whereas civil dusk twilight is the time from 30 min before sunset to 30 min after sunset. During these phases, objects can be distinguished by the naked eye, and daily outdoor activities can be performed without lighting. In contrast, nautical twilight occurs when the altitude of the sun is between 6° and 12° below the horizon, and dark and bright stars begin to appear in the sky. Astronomical twilight is a state of darkness in which the solar altitude is between 12° and 18° below the horizon. In addition, the illuminances (lx) of the astronomical and nautical twilights vary between 0.001 and 5 lx. However, the illuminance of civil twilight ranges from 5 to 1000 lx, making it possible to distinguish ships with the naked eye [31]. In general, illuminance varies according to the solar altitude.

Therefore, in this study, daytime and nighttime tracking data were classified based on the dawn and dusk times of the civil twilight phase [30]. The twilight time varies depending on the location, date, and time of the vessel sailing [30]. Using the Astral Python package, this study classified ship trajectories into day or night periods. Astral Python uses solar-earth geometrical calculations to determine the exact twilight time based on geographic coordinates, including latitude and longitude, and a given date comprising the day, month, and year [13].

Subsequently, daytime track data were allocated using a Geohash geocoding system to extract areas with high vessel traffic densities. A geohash divides space into grid forms and uses string codes instead of latitude and longitude ranges for each grid. It is a hierarchical spatial data structure that can express various levels of geographic precision by zooming in or out by removing or adding characters, respectively, at the end of a code [14,15].

A geohash divides the longitude and latitude into two, and alternately expresses them in bits. For illustrative purposes, Fig. 1 shows the process of mapping and encoding the bits collected by repeating the division a certain number of times for each character using a 5-bit unit ($2^5 = 32$) base 32 as described by the Seoul City Hall. For example, considering 32 characters from 0 to 9 and A to V, 00000 is converted to 0, 00001 to 1, and 11,111 to V. Because a Geohash can express a specific spatial range, it is a practical expression method for spatial aggregation.

In our case, by tallying the cumulative travel distances of the vessels heading for each grid, it was possible to extract the geohash grid in the concentrated area of vessel traffic and identify the main traffic flow in areas where the vessels were concentrated. To extract the geohash grid in the concentrated area of vessel traffic, the cumulative

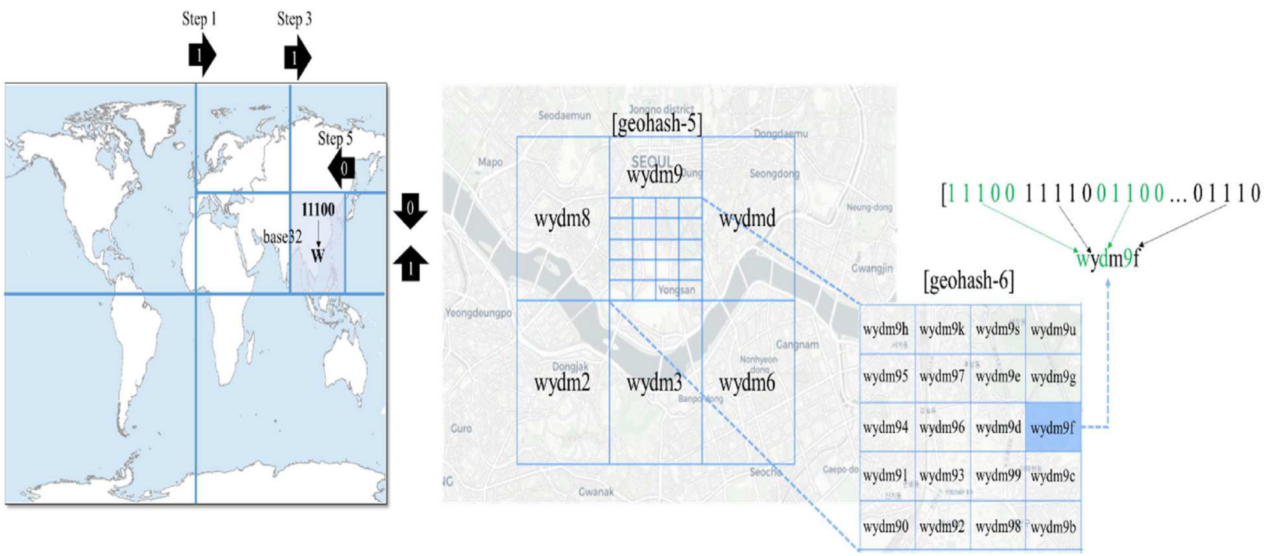

Fig. 1. The Geohash encoding concept.

distance traveled through each grid was considered using the procedure described in the following steps.

3.2. Accumulated distance traveled by vessels in each geohash grid

To evaluate the accumulated distance traveled by the vessels in each geohash grid, we estimated the distance traveled by each ship using Equation (1). This equation, the Haversine formula, calculates the straight-line distance between two points on a spherical surface [32].

$$d_i = 2r\,arcsin\left(\sqrt{sin^2\left(\frac{\varphi_{i+1}-\varphi_i}{2}\right)+cos(\varphi_i)cos(\varphi_{i+1})sin^2\left(\frac{\lambda_{i+1}-\lambda_i}{2}\right)}\right) \quad (1)$$

where r is the radius of the Earth, φ_i is the latitude of the vessel in the ith trajectory record, and λ_i is the longitude of the vessel in the ith trajectory record.

To avoid calculating the moving distances of vessels anchored or berthed waiting for engine repair or another intervention, the equation was used only for track data with speeds exceeding one knot. In addition, there was a problem due to obtaining an excessive travel distance owing to the rapid movement of the location caused by a GPS failure in some vessels. To address this problem, the maximum navigating distance over 10 s was filtered for 0.1 nm, and the maximum navigating distance per day was set to 1000 nm based on a maximum speed of 40 knots. The cumulative movement distance d_g for each grid was calculated using Equation (2).

$$d_g = \sum_{k=1}^{K}\sum_{j=1}^{J}\sum_{i=1}^{I} d_{i,j}^{k} \quad (2)$$

where K is the total collection duration of the ship trajectory data, J is the total number of ships sailing in the grid on the kth day, I is the total number of trajectory records for the jth ship on the kth day, and $d_{i,j}^{k}$ is the distance between the ith and i+1st trajectories for the jth ship on the kth day.

Subsequently, using the above equations, we can calculate the cumulative distance traveled in each grid and extract the geohash grid in a concentrated area of vessel traffic. The top 10 % of the grid with the highest cumulative travel distance was set as the main traffic density area for the vessels.

3.3. Arrangement of LFX areas

To arrange the LFX areas, they were converted into geohashes. To convert all existing locations in the LFX areas into geohash strings, the Shapley geometry package was used to generate approximately 50,000 random locations in the polygonal shape of each LFX area in an even distribution [33]. The generated location was converted into a geohash string, and unique strings were extracted from the duplicate strings.

Then, areas where the vessel traffic concentration and LFX areas coincided by more than 70 % were selected for relocation. A decrease in the threshold value results in the selection of more LFX areas for relocation. Conversely, fewer LFX areas are chosen for relocation when the threshold value is increased. The selected LFX areas were relocated to areas with the lowest coincidence rate using a grid search. A grid search was conducted, in which the polygons of the LFX area that required rearrangement were shifted at intervals of 1 nm by setting the search range to 10 nm left and right in the longitudinal direction and 10 nm up and down in the latitudinal direction.

Additionally, the search range may be adjusted if it is adjacent to land or other countries. Among the search candidates, the selected LFX areas were relocated to locations with the lowest coincidence rates.

4. Results and discussion

In this study, we used as a case study the arrangement of LFX areas established along the coasts of South Korea.

4.1. Vessel traffic-concentrated areas

A total of 59 sea-based LFX areas have been established along the South Korean coast [11]. According to the Korea Coast Guard maritime shooting training zone map (462 charts) published by the Korean Hydrographic and Oceanographic Agency, 59 LFX areas consisting of 24 areas for the Navy, 15 for the Korean Coast Guard, 13 for the Air Force, 6 for the Agency for Defense Development, and 1 for the Army are distributed, as shown in Fig. 2 [11].

The ten-day tracking data from May 1 to May 10, 2019, were used to analyze the areas with concentrated vessel traffic. Figure 3 shows the areas with concentrated vessel traffic based on Geohash-6. Observe that ship traffic was concentrated in the Southeast Sea and the West Sea area [11,34–36].

Regarding this topic, Table 1 lists the coincidence rate comparing the number of ship traffic grids based on Geohash-6. The total number of grids in the LFX area R-143 was 229, and the number of traffic-concentrated grids was 229. Consequently, the coincidence rate was 100 %. The total number of grids in the LFX area, R-100, was 220, the number of traffic-concentrated grids was 167, and the coincidence rate was 75.9 %.

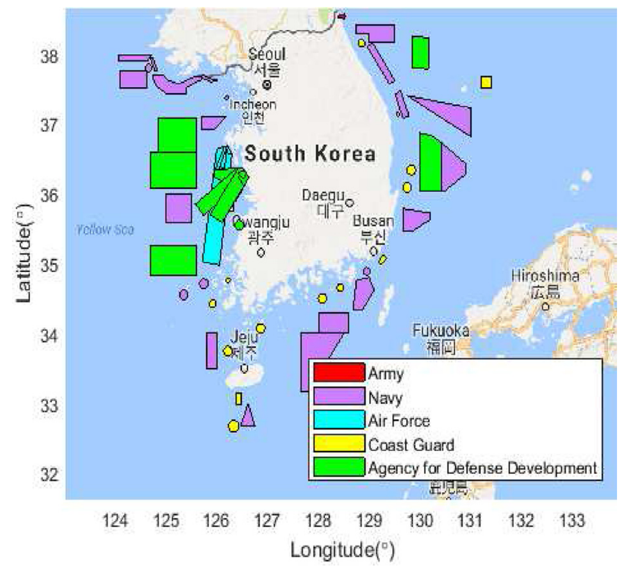

Fig. 2. Location of the LFX areas along the South Korean Coast.

4.2. Arrangement of LFX areas

As shown in Fig. 4(a), the existing LFX area at sea, R-143, was searched at intervals of one mile up, down, left, and right, while maintaining the polygonal shape. Considering the adjacent land, the search range was set to 10 nm left and right in the longitudinal direction and from −5 to +2 nm up and down in the latitudinal direction based on the previously established LFX areas. The solid purple line represents the grid search shifted at one nm intervals, the solid white line represents the LFX area at sea, and the solid yellow line represents the relocated position of the area with the lowest coincidence rate. Figure 4(b) shows that the existing LFX area R-100 was searched at intervals of one mile up, down, left, and right while maintaining a circular shape. The search range was set from −10 to +10 nm left and right in the longitudinal direction and from −10 to +4 nm up and down in the latitude direction.

Table 2 presents a comparison of the coincidence rates with the ship traffic density areas before and after the relocation of the LFX areas based on Geohash-6. Three LFX areas with a coincidence rate of more than 70 % were relocated to ensure the safety of passing ships and maintain national security [37–39]. The coincidence reduction rate was 27.9–55.3 %. Before relocation, the coincidence rate was 100 % in the R-143 LFX area. After relocation, the coincidence rate decreased to 44.7 %. The coincidence rates before and after relocating the R-100 LFX area were 75.9 % and 54.7 %, respectively.

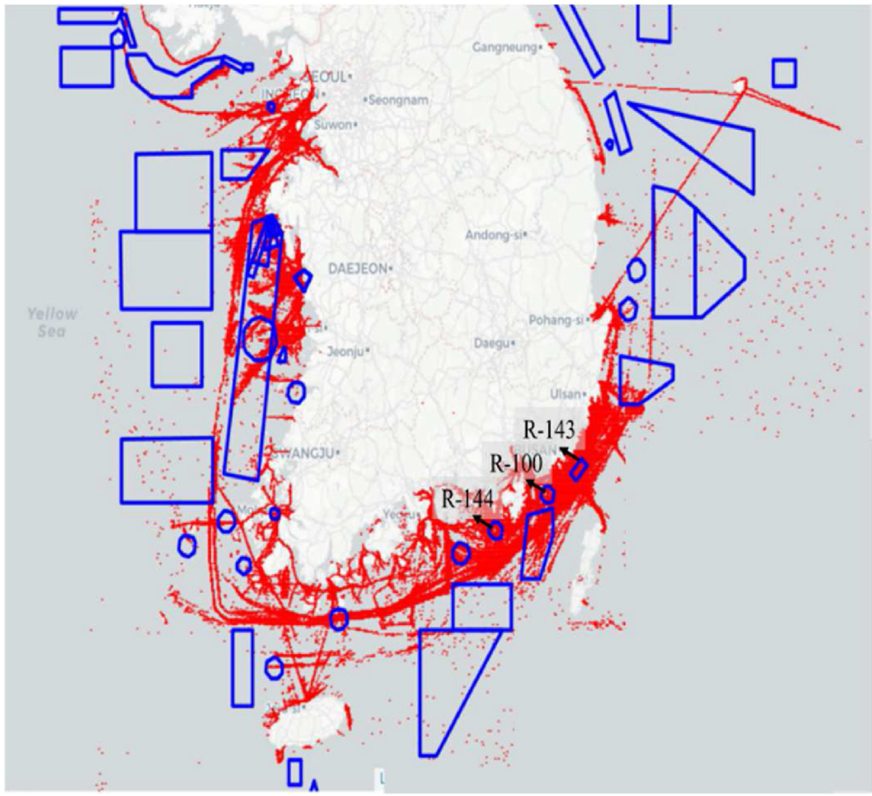

Fig. 3. Ship traffic density based on Geohash-6.

Table 1. Coincidence rate based on Geohash-6 for LFX areas.

LFX areas	Total grids	Number of traffic concentrated grids	Coincidence rate (%)
R-143	229	229	100
R-144	223	178	79.8
R-100	220	167	75.9

Table 2. Comparison of the coincidence rates before and after the relocation of LFX areas.

LFX areas	Coincidence rate before relocation (%)	Coincidence rate after relocation (%)	Coincidence reduction rate (%)
R-143	100	44.7	55.3
R-144	79.8	48.6	39.1
R-100	75.9	54.7	27.9

4.3. Discussion

The results indicate that the methodology presented in this study can be used as a guideline for designing safe live-fire exercise areas over the South Korean Coast. However, the main limitation of this study was the lack of previously published studies on the appropriate placement of LFX. This prevented us from comparing our results with those of

Fig. 4. Relocation of LFX areas: (a) R-143, (b) R-100.

previous studies. Future studies on this topic should aim to exploit the benefits of intelligent technologies in predicting safe LFX locations. It would also be worthwhile to conduct surveys and collect feedback on the effectiveness of reorganizing LFX areas using our methodology and other possible alternatives [40,41].

5. Conclusion

LFX areas threaten the safety of vessels passing through and fishermen because unexploded ordnances can be caught in fishing nets, endangering the lives of fishermen. Accordingly, an LFX area must satisfy the minimum conditions for national security training while guaranteeing maximum fishing and navigation rights. Therefore, we proposed a method for the safe and effective arrangement of LFX areas at sea.

In summary, the proposed method identified whether LFX areas coincided with areas with concentrated ship traffic. First, the ship coordinate was classified as day or nighttime based on civil twilight. And then, the ship coordinates for daytime was converted to geohash. Next, the cumulative distance in each geohash grid was used to extract the concentrated areas with vessel traffic. These areas with concentrated vessel traffic were compared with the LFX areas to determine the coincidence rates. Areas with coincidence rates exceeding a threshold value were selected for relocation. Last, the LFX area requiring relocation was moved within the established search range using a one-mile interval and relocated to the location with the least coincidence between the search candidates.

The proposed method could be improved and made more realistic and valuable by conducting surveys and collecting feedback on real-life results. In addition, consultations with organizations related to maritime activities are required to ensure that the MSP resets military activity zones. Additionally, the proposed method can be adapted and used in other countries where LFX is performed at sea.

Acknowledgments

This study was supported by the 2022 Our Sea Field Research Support Project commissioned by the Korea Maritime Institute (KMI).

Conflicts of interest

There is no conflict of interest.

References

[1] Parry C. Maritime operations and missions: the falklands case. In: From the North Atlantic to the South China sea nomos verlagsgesellschaft mbH & Co. KG; 2021. p. 321–36.
[2] STRIKFORNATO and U.S. Sixth fleet commence complex air and missile Defense exercise [Cited 7 June 2023]. Available from: https://sfn.nato.int/newsroom/2021/strikfornato-and-us-sixth-fleet-commence-complex-air-and-missile-defense-exercise.
[3] Mastro OS. Russia and China team up on the Indian ocean [Cited 6 June 2023]. Available from: https://www.lowyinstitute.org/the-interpreter/russia-china-team-indian-oce.
[4] Wishnick E, Barria C. Russia and China go sailing [Cited 7 June 2023]. Available from: https://www.foreignaffairs.com/articles/china/2015-05-26/russia-and-china-go-sailing.
[5] Cho S. China's quiet challenges at sea: explaining China's maritime activities in the Yellow Sea, 2010–2020. Asian Secur 2021;17(3):294–312. 2021.
[6] South Korea conducts largest live-fire joint military drills with U.S [Cited 7 June 20213]. Available from: https://tvpworld.com/70097350/south-korea-conducts-largest-live-fire-joint-military-drills-with-us.
[7] Japan Self-Defense Force conducts large-scale live-fire drills [Cited 5June 2023]. Available from: https://www3.nhk.or.jp/nhkworld/en/news/20230527_11/.
[8] Korean hydrographic and oceanographic agency [Cited 18 October 2022]. Available from: http://www.khoa.go.kr/eng/Main.do.
[9] Bitan VE, Călin V. Evaluation systems for antiaircraft artillery and surface-to-air live firing activities. Rev Air Force Acad 2016;14:31–8.
[10] Wehner D, Frey T. Offshore unexploded ordnance detection and data quality control. A guideline. IEEE J Sel Top Appl Earth Obs Rem Sens 2022;15:7483–98.
[11] Cooper N, Cooke S. Risky business: dealing with unexploded ordnance (UXO) in the marine environment. In: Coasts, marine structures and breakwaters 2017: realising the potential. ICE Publishing; 2018. p. 157–67.
[12] Howard B, Aker J, Reid M. Risk management for unexploded ordinance (UXO) in the marine environment. Dalhousie J Interdiscip Manag 2012;8(2).
[13] Packages for python: astral [Cited 16 October 2022]. Available from: https://repology.org/project/python:astral/packages.
[14] Morton GM. A computer oriented geodetic data base and a new technique in file sequencing. Ottawa: IBM Ltd.; 1966.
[15] Balkić Z, Šoštarić D, Horvat G. GeoHash and UUID identifier for multi-agent systems. In: International K, editor. Lecture notes in computer science symposium on agent and multi-agent systems: technologies and applications; 2012. p. 290–8.
[16] Retzlaff R, LeBleu C. Marine spatial planning: exploring the role of planning practice and research. J Plann Lit 2018;33:466–91.
[17] Fang Q, Zhu S, Ma D, Zhang L, Yang S. How effective is a marine spatial plan: an evaluation case study in China. Ecol Indicat 2019;98:508–14.
[18] Chalastani VI, Tsoukala VK, Coccossis H, Duarte CM. A bibliometric assessment of progress in marine spatial planning. Mar Pol 2021;127:104329.
[19] de Vrees Ld. Adaptive marine spatial planning in The Netherlands sector of the North Sea. Mar Pol 2021;132:103418.
[20] Põnarbaşõ K, Galparsoro I, Borja Á, Stelzenmüller V, Ehler CN, Gimpel A. Decision support tools in marine spatial planning: present applications, gaps and future perspectives. Mar Pol 2017;83:83–91.

[21] Guerreiro J. The blue growth challenge to marine governance. Front Mar Sci 2021;8:1–16.
[22] Lee SW. Impact of marine shooting range on the surrounding environment. PhD thesis. University of Kwangwoon; 2009. p. 1–155.
[23] Jung JW, Moon HS, Nam KP. An environmental management protocol for the mitigation of contaminants migration from military operational ranges. J Soil Groundwater Environ 2015;20:8–18.
[24] Lee SW, Kim HS, Jeong SJ. Measurement of noise and evaluation of noise control methods for military rifle shooting ranges. J Korea Inst Mil Sci Technol 2008;12:123–32.
[25] Baek SH, Lee AY, Park HJ, Lee WS, Choi KS. Study on the method to improve a maritime safety by analysing the distribution characteristics of the ships on marine firing range. J Korean Soc S Af 2020;35:79–85.
[26] AbuAlhaol I, Falcon R, Abielmo R, Petriu E. Mining port congestion indicators from big AIS data. In: 2018 International joint conference on neural networks (IJCNN). IEEE; 2018. p. 1–8.
[27] Wijaya WM, Nakamura Y. Predicting ship behavior navigating through heavily trafficked fairways by analyzing AIS data on Apache HBase. In: 2013 first International symposium on computing and networking. IEEE; 2013. p. 220–6.
[28] Cheraghchi F, Abualhaol I, Falcon R, Abielmona R, Raahemi B, Petriu E. Big-data-enabled modelling and optimization of granular speed-based vessel schedule recovery problem. In: 2017 IEEE International conference on big data (big data). IEEE; 2017. p. 1786–94.
[29] Wang G, Meng J, Han Y. Extraction of maritime road networks from large-scale AIS data. IEEE Access 2019;7: 123035–48.
[30] Yoo SL, Jung CY. Statistical analysis of ship collision accidents by day and night times. J Korean Soc Mar Environ Saf 2018;24:339–45.
[31] Beier P. Effects of artificial night lighting on terrestrial mammals. Ecol Consequences Artif Night Lighting 2006: 19–42.
[32] Chopde NR, Nichat M. Landmark based shortest path detection by using A* and Haversine formula. Int J Innov Res Comput Commun Eng 2013;1:298–302.
[33] Shapely package [Cited 20 October 2022]. Available from: https://pypi.org/project/shapely.
[34] Kim DW, Park JS, Park YS. Comparison analysis between the IWRAP and the ES model in ulsan water way. J Navig Port Res 2011;35(4):281–7.
[35] Song SC, Park Sh, Yeo GT. Network structure analysis of a sub-hub-oriented port. The Asian J Ship Ping Logist 2019; 35(2):118–25.
[36] Lee H, Park D, Choo S, Pham HT. Estimation of the non-greenhouse gas emissions inventory from ships in the port of Incheon. Sustainability 2020;12(19):8231.
[37] Irshaid H, Hasan MM, Hasan R, Oh JS. User activity and trip recognition using spatial positioning system data by integrating the Geohash and Gis approaches. Transport Res Rec 2021;2675(4):391–405.
[38] Xiang W. An efficient location privacy preserving model based on Geohash. In: 6th International conference on behavioral, economic and socio-cultural computing (BESC). IEEE Publications; 2019. p. 1–5.
[39] Davis N, Raina G, Jagannathan K. A multi-level clustering approach for forecasting taxi travel demand. In: 19th international conference on intelligent transportation systems (ITSC). IEEE Publications; 2016. p. 223–8.
[40] Chen NY, Shaw J, Lin H. Exploration method improvements of autonomous robot for a 2-d environment navigation. J Mar Sci Technol 2017;25(1).
[41] Kao SL, Chang KY, Hsu TW. Fuzzy grounding alert system for vessel traffic service via 3d marine Gis. J Mar Sci Technol 2017;25(2). 2017.